

The Interpretation and Implication of the Afterglow of GRB 060218

Yizhong Fan^{1,2,3*}, Tsvi Piran¹ † and Dong Xu⁴

¹The Racah Inst. of Physics, Hebrew University, Jerusalem 91904, Israel

²Purple Mountain Observatory, Chinese Academy of Science, Nanjing 210008, China

³National Astronomical Observatories, Chinese Academy of Sciences, Beijing 100012, China

⁴Dark Cosmology Centre, Niels Bohr Institute, University of Copenhagen, Juliane Maries Vej 30, 2100 Copenhagen, Denmark

Accepted Received; in original form

ABSTRACT

The nearby GRB 060218/SN 2006aj was an extremely long, weak and very soft GRB. While it was peculiar in many aspects its late ($> 10^4$ sec) X-ray afterglow showed a canonical power law decay. Assuming that this component arises due to a relativistic blast wave decelerated by a circumburst matter we infer that the blast wave’s kinetic energy was rather high, 5×10^{50} erg, close to what is seen in other GRBs. The lack of a “jet break” implies that the outflow was wide $\theta_j \sim 1$. The rather weak early optical emission rules out a dense circumburst wind profile. It also constrains the initial Lorentz factor to be significantly lower than usual, $\Gamma_{\text{ini}} \sim 15$. The observed afterglow suggests that the medium surrounding a massive star progenitor (up to distances of $\sim 10^{17} - 10^{18}$ cm) is not the expected dense stellar wind (a similar result was seen in many other bursts and in particular in GRB 030329). This implies that the progenitor’s wind was weak during the last 100-1000 years before the burst. This interpretation requires a different source for the thermal emission seen in the early X-ray and late optical/UV. We speculate that this emission arises from the interaction of the relativistic ejecta with the stellar envelope.

Key words: Gamma Rays: bursts—ISM: jets and outflows—radiation mechanisms: nonthermal—X-rays: general

1 INTRODUCTION

GRB 060218 (Cusumano et al. 2006a) was a nearby ($z=0.033$, Mirabal & Halpern 2006; Cusumano et al. 2006b) burst associated with a bright type Ic broad-lines SN (Modjaz et al. 2006; Sollerman et al. 2006; Pian et al. 2006; Mirabal et al. 2006). It is distinguished in several aspects from other bursts: (i) It is very long ($T_{90} \sim 2000$ sec). (ii) The prompt γ -ray and X-ray luminosity is extremely low $\sim 10^{47}$ erg s⁻¹ (Sakamoto et al. 2006) and the overall isotropic equivalent γ -ray energy, a few $\times 10^{49}$ erg, is small compared to typical bursts. (iii) The prompt emission is very soft and it contains a soft thermal component in the X-ray band. The thermal emission begins at ~ 152 sec and continues up to $\sim 10^4$ sec. (iv) A second thermal component in the UV/optical band peaks at $t \sim 10^5$ sec after the GRB trigger (Campana et al. 2006). (v) For $t > 10^4$ sec, the XRT lightcurve is simple and is well described a single power-law

decay $t^{-1.15}$ with no break (Campana et al. 2006). While the prompt emission is very different from a typical GRB and the optical emission is complicated by the appearance of the thermal bump and the supernova signal this last component, the X-ray afterglow, is rather typical.

We focus here on this X-ray afterglow, which can be interpreted in terms of the standard afterglow model, and use it as a key to understand what has happened in this burst. One can infer from it the kinetic energy, $E_k \sim 5 \times 10^{50}$ erg, as well as the wide opening angle, $\theta_j \sim 1$, of the relativistic component of the ejecta. One can also infer, from a combined analysis of this and the optical afterglow that the initial Lorentz factor was rather small as compared to typical GRBs.

The association with a type Ic SN suggests that the progenitor was a WR-star (Campana et al. 2006). One expects, therefore, that the central engine is surrounded by a dense stellar wind, like the one seen in GRB 980425 that was associated with SN 98bw (Li & Chevalier 1999; Waxman 2004). However, the density nearest to the progenitor depends on the mass loss rate during the latest phases of the

* Lady Davis Fellow, E-mail: yzf@pmo.ac.cn

† tsvi@phys.huji.ac.il

WR-star, which is unknown at present (Woosley, Zhang & Heger 2003). Using the X-ray and optical data we show that the circumburst medium surrounding the progenitor has a constant low density. Since the ejecta is very wide this conclusion cannot be attributed to anisotropy in the mass loss as has been suggested for GRB 030329¹.

The low luminosity of the prompt emission as well as the soft spectrum might be attributed to a viewing angle. This possibility has been questioned by Nousek et al. (2006). We show (in sec. 3) that while such a model is compatible with the X-ray and optical afterglow light curves (for a constant density circumburst matter profile) it requires a very large prompt energy as well as a very large ratio of prompt energy to kinetic energy. Furthermore, the small ratio of the offset viewing angle to the jet opening angle makes this interpretation unlikely.

We examine possible sources for the thermal emission in section 4. Our conclusions and the implications for the GRB/SN connection are discussed in section 5.

2 THE MULTI-WAVELENGTH AFTERGLOW

The late ($> 10^4$ sec) X-ray afterglow is similar to the one seen in typical GRBs in its overall intensity as well as in the almost standard power law decay index. In the standard GRB afterglow model (Sari, Piran & Narayan 1998; Piran 1999), the X-ray afterglow is produced by a blast wave that is slowed down by a constant density circumburst medium. The bulk Lorentz factor is:

$$\Gamma \approx 3.4 E_{k,51}^{1/8} n_0^{-1/8} t_d^{-3/8} (1+z)^{3/8}, \quad (1)$$

where n is the number density of the surrounding matter, and t_d is the observer's time in days. The lack of a "jet-break" (Rhoads, 1999; Sari et al, 1999; Halpern et al., 1999) in the X-ray afterglow lightcurve in the range $t \sim 0.1 - 10$ days suggests a very wide opening angle:

$$\theta_j > 1/\Gamma(t_d = 10) = 0.7 E_{k,51}^{-1/8} n_0^{1/8} t_{d,1}^{3/8} (1+z)^{-3/8}. \quad (2)$$

The emission of the shock is determined by the peak flux, $F_{\nu, \max}$ and by the synchrotron and cooling frequencies, ν_m and ν_c (Sari, Piran & Narayan 1998; Yost et al. 2003):

$$F_{\nu, \max} = 63.9 \text{ mJy } (1+z) D_{L,26.7}^{-2} \epsilon_{B,-2}^{1/2} E_{k,51} n_0^{1/2}, \quad (3)$$

$$\nu_m = 5.4 \times 10^{10} \text{ Hz } E_{k,51}^{1/2} \epsilon_{B,-2}^{1/2} \epsilon_{e,-1}^2 C_p^2 (1+z)^{1/2} t_d^{-3/2}, \quad (4)$$

$$\nu_c = 2 \times 10^{16} \text{ Hz } E_{k,51}^{-1/2} \epsilon_{B,-2}^{-3/2} n_0^{-1} (1+z)^{-1/2} t_d^{-1/2} \frac{1}{(1+Y)^2}, \quad (5)$$

where D_L is the corresponding luminosity distance, p is the power-law index of the shocked electrons, we use $p = 2.3$ throughout this work, and $C_p \equiv 13(p-2)/[3(p-1)]$. $Y = (-1 + \sqrt{1 + 4\eta\eta_{KN}\epsilon_e/\epsilon_B})/2$ is the Compton parameter, where $\eta = \min\{1, (\nu_m/\nu_c)^{(p-2)/2}\}$ (Sari, Narayan &

Piran 1996; Wei & Lu 1998), $0 \leq \eta_{KN} \leq 1$ is a coefficient accounting for the Klein-Nishina effect (Fan & Piran 2006).

The flux recorded at $t_d = 0.1$ by XRT, $\mathcal{F} = 2 \times 10^{-11} \text{ ergs s}^{-1} \text{ cm}^{-2}$, should be compared with the theoretical prediction (assuming the XRT energy range $\nu_X > \max\{\nu_c, \nu_m\}$):

$$\begin{aligned} \mathcal{F} &= \int_{\nu_{X1}}^{\nu_{X2}} F_{\nu_X} d\nu_X \\ &= 1.4 \times 10^{-10} \text{ ergs s}^{-1} \text{ cm}^{-2} (1+z)^{(p+2)/4} D_{L,26.7}^{-2} \\ &\quad \epsilon_{B,-2}^{(p-2)/4} \epsilon_{e,-1}^{p-1} E_{k,51}^{(p+2)/4} (1+Y)^{-1} t_{d,-1}^{(2-3p)/4}, \end{aligned} \quad (6)$$

where $\nu_{X1} = 0.2 \text{ keV}$ and $\nu_{X2} = 10 \text{ keV}$. The agreement suggests that the typical parameters used here are consistent with the observation.

While the X-ray afterglow after 10^4 sec seem regular the optical and ultraviolet afterglows are very peculiar. The early data ($t_d \leq 0.02$) seems to be the low energy tail of the prompt X-ray/ γ -ray non-thermal emission. On the other hand the late long-wavelength afterglow ($0.4 < t_d < 1.4$) is also dominated by a thermal component (Campana et al. 2006). With the extinction correction (Guenther et al. 2006), the spectral index of the UVB emission, at this time, is about 2 for $\nu < 10^{15} \text{ Hz}$.

If $\Gamma_{\text{ini}} > 35$, the V-band afterglow should peak at $t_d \sim 0.002$ (see eq.[1]) with a flux $\sim 64 \text{ mJy } \epsilon_{B,-2}^{1/2} E_{k,51} n_0^{1/2}$. This is much stronger than the observed flux (see Fig.1). A possible resolution of this contradiction is that the initial Lorentz factor is small $\Gamma_{\text{ini}} \sim 15$. In this case the UV/optical afterglow peaks at $t_d \sim 0.06$. The V-band flux should be

$$\begin{aligned} F_{\nu_V}^w &\approx 0.1 \text{ mJy } (1+z)^{\frac{p+3}{4}} D_{L,26.7}^{-2} E_{k,51}^{\frac{p+3}{4}} n_0^{1/2} \epsilon_{e,-1}^{p-1} C_p^{p-1} \\ &\quad \epsilon_{B,-2}^{\frac{p+1}{4}} t_d^{\frac{-3(p-1)}{4}}. \end{aligned} \quad (7)$$

Note that a factor $1/64$ has been taken into account when evaluating $F_{\nu, \max}$ since the radius of the shock front satisfies $R \approx 2\Gamma^2 ct$ rather than $R \approx 8\Gamma^2 ct$ for $t_d < 0.06$. This flux is compatible with the observations.

Fig. 1 depicts a comparison of the theoretical the multi-wavelength afterglow lightcurves with the observations. Here the synchrotron-self-absorption effect has been taken into account but the external Inverse Compton cooling of the shocked electrons, caused by the long term prompt X-ray/ γ -ray emission, has not. Such a simplification is mainly for the reduction of the calculation. Therefore, both the X-ray and the optical emission at $t < 0.1$ day have been overestimated. The actual fluxes should be lower, which are consistent with the observations. The initial Lorentz factor ($\Gamma_{\text{ini}} \sim 15$) used to avoid a strong early optical emission is significantly lower than typical Lorentz factors inferred in GRBs. Γ_{ini} cannot be much smaller than this value. The X-ray flux declines as a single power-law at $t \sim 9 \times 10^3$ sec, implies that the blast wave obtained the Blandford-McKee profile at this stage. This poses a lower limit on the initial Lorentz factor of the outflow of $\Gamma > 8 E_{k,51}^{1/8} n_0^{-1/8} t_{d,-1}^{-3/8}$.

In the stellar wind model (Dai & Lu 1998; Mészáros, Rees & Wijers 1998), $n = 3 \times 10^{35} A_* R^{-2} \text{ cm}^{-3}$, where $A_* = [\dot{M}/10^{-5} M_\odot \text{ yr}^{-1}][v_w/(10^8 \text{ cm s}^{-1})]$ (Chevalier & Li 2000), \dot{M} is the mass loss rate of the progenitor, v_w is the velocity of the wind. The bulk Lorentz factor of the outflow can

¹ The optical afterglow of GRB 030329 can be fitted reasonably well with a constant density model (e.g., Berger et al. 2003a; Huang, Cheng & Gao 2006). However, the ejecta of GRB 030329 is very narrow (~ 0.05 rad) and the ISM-like medium may be caused by an anisotropic mass loss of the progenitor (Woosley et al. 2003).

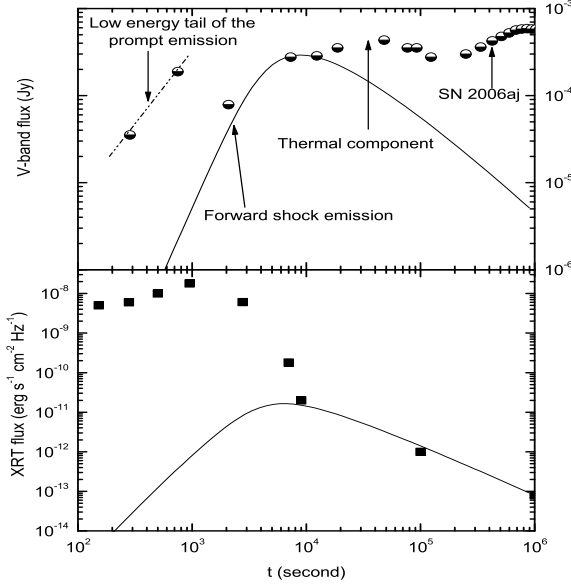


Figure 1. A comparison of the observed (Campana et al. (2006)) XRT and V-band afterglow lightcurves of GRB 060218 with the (numerical) predictions for the forward shock emission in the constant density circumburst medium (solid line). The parameters used are: $E_k = 5 \times 10^{50}$ erg, $\Gamma_{\text{ini}} = 15$, $\theta_j = 1$, $\epsilon_e = 0.1$, $\epsilon_B = 0.01$, $n = 0.5 \text{ cm}^{-3}$ and $p = 2.3$.

be estimated by (the superscript “w” represents the wind model):

$$\Gamma^w \approx 2E_{k,51}^{1/4} A_*^{-1/4} t_d^{-1/4} (1+z)^{1/4}. \quad (8)$$

Following Chevalier & Li (2000) the equations that govern the forward shock emission are:

$$F_{\nu, \text{max}}^w = 1.4 \text{ Jy} (1+z)^{3/2} \epsilon_{B,-2}^{1/2} E_{k,51}^{1/2} A_* t_d^{-1/2} D_{L,26.7}^{-2}, \quad (9)$$

$$\nu_m^w \approx 4 \times 10^{10} \text{ Hz} \epsilon_{e,-1}^2 C_p^2 E_{k,51}^{1/2} \epsilon_{B,-2}^{1/2} (1+z)^{1/2} t_d^{-3/2}, \quad (10)$$

$$\nu_c^w \approx 10^{14} \text{ Hz} \epsilon_{B,-2}^{-3/2} E_{k,51}^{1/2} A_*^{-2} (1+z)^{-3/2} t_d^{1/2} (1+Y)^{-2}. \quad (11)$$

We estimate the expected XRT energy flux as:

$$\begin{aligned} \mathcal{F}^w &\approx 1.8 \times 10^{-10} \text{ erg s}^{-1} \text{ cm}^{-2} \epsilon_{B,-2}^{\frac{p-2}{4}} E_{k,51}^{\frac{p+2}{4}} t_{d,-1}^{\frac{-(3p-2)}{4}} \\ &D_{L,26.7}^{-2} \epsilon_{e,-1}^{p-1} C_p^{p-1} (1+z)^{\frac{p+2}{4}} (1+Y)^{-1}. \end{aligned} \quad (12)$$

The canonical value is a few times that of the XRT observation of GRB 060218 $\sim 2 \times 10^{-11} \text{ erg s}^{-1} \text{ cm}^{-2}$ at $t_d \sim 0.1$ (note that $Y \sim \text{a few}$). On the other hand, assuming $\nu_V > \max\{\nu_c^w, \nu_m^w\}$, the V-band flux is:

$$\begin{aligned} F_{\nu_V}^w &\approx 22 \text{ mJy} \epsilon_{B,-2}^{\frac{p-2}{4}} E_{k,51}^{\frac{p+2}{4}} t_{d,-1}^{\frac{-(3p-2)}{4}} \\ &D_{L,26.7}^{-2} \epsilon_{e,-1}^{p-1} C_p^{p-1} (1+z)^{\frac{p+2}{4}} (1+Y)^{-1}. \end{aligned} \quad (13)$$

If we normalize \mathcal{F}^w as $\sim 2 \times 10^{-11} \text{ erg s}^{-1} \text{ cm}^{-2}$ then $F_{\nu_V}^w \sim 3 \text{ mJy}$, which is brighter by a factor of 10 than the observed flux $\sim 0.3 \text{ mJy}$. In other words, a contrast between V-band flux and the X-ray flux smaller than $\mathcal{R} \equiv F_{\nu_V}^w / F_{\nu_X}^w \approx (\nu_X / \nu_V)^{p/2}$ is needed. This could be, for example, $\nu_X > \nu_c^w > \nu_V$ and $\nu_c^w \sim 100\nu_V \sim 5 \times 10^{16} \text{ Hz}$ at $t_d \sim 0.1$, requiring a very small A_* (~ 0.01) and/or very small ϵ_B ($\sim 10^{-5}$). In this case, we have $F_{\nu_V}^w / F_{\nu_X}^w = (\nu_X / \nu_c^w)^{1/2} (\nu_X / \nu_V)^{(p-1)/2} \sim 0.1\mathcal{R}$, which is

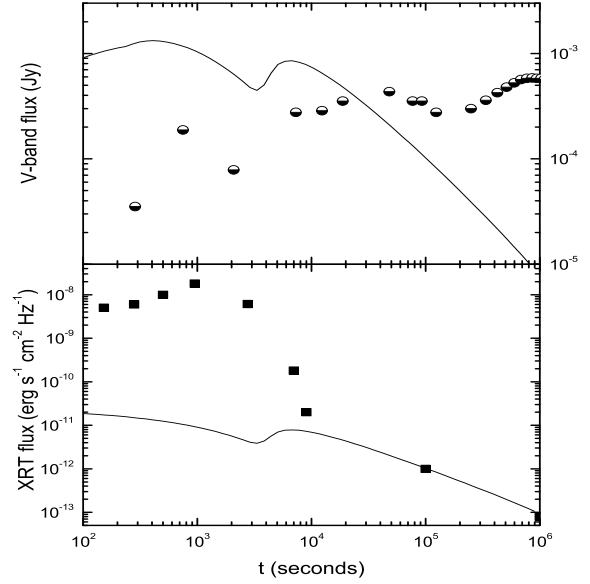


Figure 2. A comparison of the observed (Campana et al. (2006)) XRT and V-band afterglow lightcurves of GRB 060218 with the (numerical) predictions for the forward shock emission in the wind case (solid line). The parameters used are: $E_k = 10^{51}$ erg, $\Gamma_{\text{ini}} = 4$, $\theta_j = 1$, $\epsilon_e = 0.2$, $\epsilon_B = 0.01$, $A_* = 1$ and $p = 2.3$. The troughs are caused by the external inverse Compton cooling. As shown in the upper panel, the wind model is incompatible due to its too bright optical emission.

compatible with the data. However, this is unlikely because $\nu_c^w \sim 5 \times 10^{16} \text{ Hz} t_{d,-1}^{1/2}$, which is in the XRT energy range for $t_d > 1$. The X-ray temporal and spectral indices (α_X and β_X) thus change to be $-(1-3p)/4$ and $-(p-1)/2$ rather than $-(2-3p)/4$ and $-p/2$ (Chevalier & Li 2000). Both the temporal steepening and the spectral flattening were not seen in GRB 060218. The other possible scenario is $\nu_c^w > \nu_X > \nu_V$, which also yields $F_{\nu_V}^w / F_{\nu_X}^w = (\nu_X / \nu_V)^{(p-1)/2} \sim 0.1\mathcal{R}$. But in this case, the spectral and temporal indices should be $-(p-1)/2$ and $-(1-3p)/4$ respectively. As $\alpha_X \sim -1.2$ this implies $p \sim 2$ and $\beta_X \sim -0.5$, which is inconsistent with the observed $\beta_X \sim -2.3 \pm 0.6$ at $t_d \sim 3$ (De Luca 2006). We therefore conclude that a dense wind model is unlikely.

For illustration, we compare in Fig. 2 the (numerically calculated) predicted V-band and X-ray afterglow lightcurves with the observations. Both synchrotron-self absorption and early external inverse Compton cooling, caused by the prompt γ -ray/X-ray emission, have been taken into account. To calculate the external inverse Compton cooling, we have approximated the external photon luminosity as $L_{ph} \sim 1.5 \times 10^{46} \text{ erg s}^{-1}$ for $t < 3000 \text{ s}$ and $L_{ph} \sim 1.5 \times 10^{46} \text{ erg s}^{-1} (t/3000)^{-5.2}$ for $3000 \text{ s} < t < 9000 \text{ s}$, otherwise $L_{ph} \sim 0$. The external inverse Compton parameter is calculated as $Y_{EIC} \approx U_{ph}/U_B$, where $U_{ph} = L_{ph}/(4\pi R^2 \Gamma^2 c)$, $U_B = 1.8 \times 10^{33} \text{ erg cm}^{-3} \epsilon_B \Gamma^2 R^{-2}$ is the magnetic energy density at the shock front. The troughs in Fig. 2 are caused by the external inverse Compton cooling. As expected from our analytical argument we could not find proper parameters that fit the data. The calculated early V-band flux is too bright to match the observation.

An alternative scenario suggested by Waxman (2004) for GRB 980425 is that the source of the X-ray afterglow is

a sub-relativistic outflow. However, in this case the kinetic energy of the ejecta satisfies $E_k \sim 10^{48} \text{ erg } \beta^3 A_*(t_{\text{dec}}/0.1\text{d})$, where β is the velocity of the ejecta, in units of c , t_{dec} is the deceleration timescale of the ejecta. For such small E_k ($\sim 10^{48} \text{ erg}$), it is straightforward to show that the resulting X-ray flux at $t_{\text{dec}} \sim 0.1 \text{ day}$ is 2 to 3 order lower than the data. $A_* \gg 1$ permits a much larger E_k and could give rise to X-ray emission as strong as the detected one. But the resulting UV/optical emission at t_{dec} is, once more, too bright to be consistent with the data.

We summarize this section by reiterating our conclusions. The X-ray afterglow from 10^4 sec to 10^6 sec is well fitted by a wide angle relativistic blast wave propagating into a constant density circumburst medium. The kinetic energy of the blast wave is $E_k = 5 \times 10^{50} \text{ erg}$. Considering the wide opening angle the total energy of this relativistic ejecta is comparable to the one seen in typical GRB afterglows (Panaitescu & Kumar, 2001; Frail et al. 2001; Piran et al. 2001). On the other hand the combination of the X-ray lightcurve and the earlier low optical/UV emission limits the initial Lorentz factor as $8 < \Gamma_{\text{ini}} < 15$. With this interpretation both the early ($< 10^4 \text{ sec}$) thermal X-ray emission and the late ($\sim 4 \times 10^4 - 10^5 \text{ sec}$) optical thermal emission must arise from a different component and not from the relativistic blast wave.

3 THE CONS AND PROS OF AN OFF-AXIS JET

A highly beamed emission observed off axis would result be seen as soft and weak, like in this burst. Nousek et al. (2006) argue against the possibility that GRB 060218 was a regular GRB viewed off axis. In this case the peak of the forward shock emission should be monochromatic, whereas in GRB 060218 the X-ray emission peaks at $t \leq 10^4 \text{ sec}$ and the UV/optical emission peaks at $t \sim 4 \times 10^4 \text{ sec}$. This argument becomes irrelevant if we interpret the UVOT thermal component as arising from a different source. In this scenario, the forward shock UV/optical emission peaked at $t \sim 10^4 \text{ sec}$ but the late UV/optical afterglow lightcurve is dominated by the thermal component produced by the hot expanding envelope. In this case the outflow could be an off-axis jet. Fig. 3 depicts a numerical calculation of the afterglow for an off-axis jet. The expected lightcurve is consistent with the data.

For an off-axis jet propagating into a constant density circumburst medium the detection timescale satisfies:

$$dt_{\text{off}} \approx [1 + (\Gamma\Delta\theta)^2]dt, \quad (14)$$

where $\Delta\theta$ is the angle between the line of the sight and the edge of the jet and the subscript “off” represents the off-axis case. When the flux begins to drop normally, $\Gamma \sim 1/\Delta\theta$, $t_{\text{off}} \sim 2t$ and thus

$$\Delta\theta \approx 0.1 E_{k,51}^{-1/8} n_0^{1/8} t_{\text{off},-1}^{3/8} (1+z)^{-3/8}. \quad (15)$$

The detected prompt X-ray and γ -ray energy satisfies

$$E_{\gamma,\text{obs}} \approx \frac{E_{\gamma,0}}{[1 + (\Gamma_{\text{ini}}\Delta\theta)^2]^{3/2}}, \quad (16)$$

where both energies are the isotropic equivalent energies. Now $E_{\gamma,\text{obs}} \sim 10^{50} \text{ erg}$ yields $E_{\gamma,0} \sim 10^{53} \text{ erg}$. Given the fact

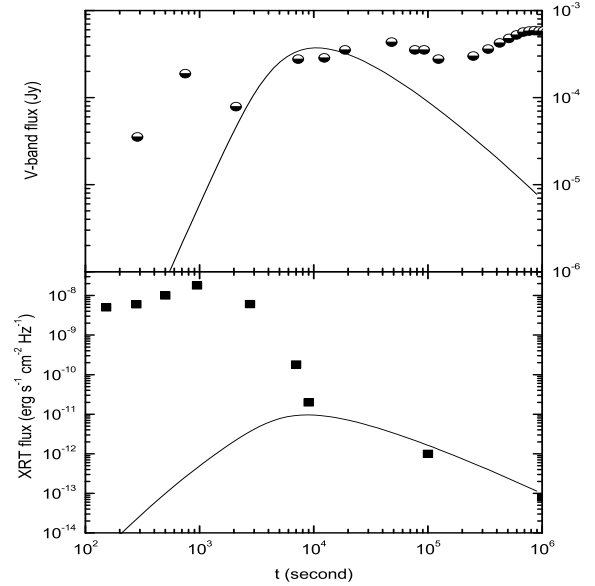


Figure 3. A comparison of the observed XRT and V-band afterglow lightcurve of GRB 060218 with the expected forward shock lightcurve of a blast wave powered by an off-axis ejecta expanding into the medium with a constant density (solid line). The parameters used are: $E_k = 10^{51} \text{ erg}$, $\Gamma_{\text{ini}} = 30$, $\theta_j = 0.6$, $\Delta\theta = 0.05$, $\epsilon_e = 0.15$, $\epsilon_B = 0.01$, $z = 0.033$, $n = 1 \text{ cm}^{-3}$ and $p = 2.3$.

that the jet is very wide this implies a total γ -ray energy $\sim 10^{53} \text{ erg}$, which is much larger than energies typically inferred in regular GRBs (Frail et al. 2001; Bloom, Frail & Kulkarni 2003). Furthermore, a comparison of the γ -ray energy with the remaining kinetic energy yields a ratio of ~ 100 , much larger than what is typically seen in regular GRBs.

A second problem with this model arises from the observation that the relation (16) yields $\Gamma_{\text{ini}}\Delta\theta \sim 3$ and thus, $\Delta\theta \sim 0.1\Gamma_{\text{ini}}^{-1}$. This “off axis” angle is much smaller than the very wide jet opening angle $\theta_j \sim 1$ indicated by the lack of a jet break in the X-ray afterglow observation. The probability for the ejecta being off-axis is much smaller than being on-axis. Similar considerations hold against an off-axis jet propagating into a circumburst wind.

4 THE THERMAL EMISSION

A soft thermal component is seen (Campana et al. 2006) in the X-ray spectrum comprising $\sim 20\%$ of the 0.3-10 keV flux. It begins at $\sim 152 \text{ sec}$ and lasts up to $\sim 10^4 \text{ sec}$. The fitted black body temperature shows a marginal decrease ($kT \simeq 0.16 - 0.17 \text{ keV}$, with k the Boltzmann constant) and a clear increase in luminosity, by a factor of 4 in the time range 300s-2600s, corresponding to an increase in the apparent emission radius from $R_{\text{BB,XRT}} = (5.2 \pm 0.5) \times 10^{11} \text{ cm}$ to $R_{\text{BB,XRT}} = (1.2 \pm 0.1) \times 10^{12} \text{ cm}$ (Campana et al. 2006). In the sharp decline phase, the XRT emission is dominated by a thermal component ($kT = 0.10 \pm 0.05 \text{ keV}$, the corresponding apparent emission radius is $R_{\text{BB,XRT}} = 6.6_{-4.4}^{+14} \times 10^{11} \text{ cm}$). This thermal component is undetectable in later XRT observation.

A second thermal component is detected by the UVOT.

At 1.4 days ~ 120 ksec the black body peak is centered within the UVOT passband. The fitted values are $kT = 3.7^{+1.9}_{-0.9}$ eV and $R_{\text{BB,UVOT}} = 3.29^{+0.94}_{-0.93} \times 10^{14}$ cm, implying an expansion speed of $(2.7 \pm 0.8) \times 10^9$ cm s $^{-1}$. This speed is typical for a supernova and it is also comparable with the line broadening observed in the optical spectra (Pian et al, 2006). The UVOT thermal component is therefore very likely dominated by the expanded hot stellar envelope (see also Campana et al. 2006).

The nature of the X-ray thermal emission is less clear. Campana et al. (2006) suggest that it arises from a shock break out from a dense wind surrounding the SN progenitor. As we have shown earlier the medium surrounding the progenitor is more likely to be constant, low density medium rather than the dense wind with a $A_* \sim 3$ required in this model (Campana et al. 2006). We suggest, therefore, that the XRT thermal component arises from a shock heated stellar matter. As the size of the emitting black body region ($6 \times 10^{11} - 10^{12}$ cm) is larger than the size of a typical WR- star (10^{11} cm) there are two possibilities: The emission could be from a hot cocoon surrounding the GRB ejecta (Ramirez-ruiz, Celotti & Rees 2002; Zhang et al. 2004) and expanding initially with $v \sim 0.1c$. An alternative possibility is that the X-ray thermal emission arises from the shock break out from the stellar envelope. This would require, however, a progenitor's size of $\sim 10^{12}$ cm. This is much larger than $\sim 10^{11}$ cm or less, that is expected from a star stripped from its H, He and probably O, as inferred from the spectroscopic analysis of the SNe (Pian et al, 2006). It is not clear if stellar evolution model can accommodate such a progenitor, but surprises of this nature have happened in the past. A relativistic radiation-hydrodynamics calculations are needed to test the viability of these two possibilities. This is beyond the scope of this work.

Here we just show that a hot and optical thick outflow could account for the temporal behavior of the XRT and UVOT thermal emission. After the central engines turns off (i.e., there is no fresh hot material injected), the hot outflow expands and cools adiabatically as $T \propto n_p^{1/3} \propto R^{-\alpha/3}$, where $\alpha = 3$ if the hot outflow is spreading and $\alpha = 2$ otherwise, n_p is the number density of the particle. Once the hot region cools adiabatically so that $kT \ll 0.2$ the thermal emission recorded by XRT in the range 0.2 to 10 keV decrease quickly with time as $L_{\text{th,XRT}} \propto R^2 e^{-0.2\text{keV}/kT} \propto R^2 e^{-\alpha R/3R_0}$, where R_0 is the radius of the outflow at the turning off time of the central engine. The V-band flux is $L_{\text{th,V}} \approx 4\pi\sigma R^2 T^4 \frac{y^3 \Delta y}{ey-1}$, where $y = 2.3\text{eV}/kT$, $\Delta y \approx 0.13y$, accounting for the FWHM width of V-band. For $y \ll 1$, $L_{\text{th,V}} \propto TR^2 \propto R^{2-\alpha/3} \propto t^{2-\alpha/3}$, increases with time until $y \sim 1$ and then it decreases rapidly. As noted by Campana et al. (2006), such a behavior is in agreement with *Swift*'s observations.

5 DISCUSSION AND SUMMARY

The recent nearby burst GRB 060218 had many peculiar features. However, after $\sim 10^4$ sec it had a rather usual X-ray afterglow lightcurve. Focusing on this lightcurve we draw the following conclusions.

- The non-thermal components of the afterglows can be

understood within the standard fireball blast wave model, provided that the overall kinetic energy is 5×10^{50} erg and it has a relatively low initial Lorentz factor.

- The lack of a “jet break” up to 10^6 sec indicates that the outflow is wide $\theta_j \sim 1$.
- The medium surrounding the progenitor has a constant, low density profile rather than the expected dense stellar wind.
- The X-ray and optical/UV thermal emission cannot arise from the relativistic ejecta. A shock heated envelope of the progenitor is the most natural source. The question whether the envelope has expanded rapidly or was it initially large is open.
- While one cannot rule out that the soft spectrum and low luminosity of GRB 060218 arose due to off-axis observations we find that this is unlikely. Such a model requires a very large total energy $\sim 10^{53}$ erg and a very large ratio of prompt γ energy to the remaining kinetic energy. Furthermore, this is improbable in view of the large opening angle of the relativistic ejecta $\theta_j \sim 1$ and the small off axis viewing angle needed $\Delta\theta \sim 0.05$.

There are several implications to these conclusions. First we note that the wide angle of the relativistic ejecta is incompatible with the usual Collapsar model, in which a narrow jet punches a narrow hole in the envelope of a WR star (Zhang et al. 2004).

Another feature that is inconsistent with the canonical version of this model is the lack of a clear wind profile. The afterglows arises at a distance of $R \sim 10^{17}$ cm from the central engine. It could be that the observed profile appeared arose from the interaction of the wind with the surrounding matter or it may reflect a low mass-loss rate of the progenitor star during the post-helium burning phases. A similar feature was seen also in GRB 030329. Further complications are the low initial Lorentz factor and above all the peculiar very soft and low luminosity prompt γ emission. This low luminosity is almost in a contrast with the fact that the total energy is comparable to the one observed in typical GRBs.

We conclude that GRB 060218 was an almost “failed GRB”. Due to some unique feature of the progenitor (a larger than usual size?) the relativistic ejecta almost did not make it across the envelope. This has lead to a wide relativistic outflow with an unusually low initial Lorentz factor. This, in turn, lead to the softer spectrum (possibly due to internal shocks taking place in a region with optical depth of order unity). A significant fraction of the energy was given to a hot cocoon and was reprocessed as a thermal emission - seen both in X-ray and later in the UV/optical. One can speculate that in many other cases the relativistic ejecta would have stopped completely and we would have a “failed GRB”. It is possible that this is the reason why GRBs are not seen in most type Ib,c SNe (Berger et al., 2003b, Soderberg et al., 2006).

ACKNOWLEDGMENTS

We thank E. Waxman for a helpful discussion. This work is supported by US-Israel BSF and by the ISF via the Israel center for High Energy Astrophysics. TP acknowledges the support of Schwartzmann University Chair. YZF is also supported by the National Natural Science Foundation (grants

10225314 and 10233010) of China, and the National 973 Project on Fundamental Researches of China (NKBRF G19990754). DX is at the Dark Cosmology Center funded by The Danish National Research Foundation.

REFERENCES

- Berger E., et al., 2003a, *Nature*, 426, 154
 Berger E., et al. 2003b, *ApJ*, 599, 408
 Bloom J. S., Frail D. A., Kulkarni S. R., 2003, *ApJ*, 594, 674
 Chevalier R. A., Li Z. Y., 2000, *ApJ*, 536, 195
 Campana S., et al., 2006, *Nature*, submitted (astro-ph/0603279)
 Colgate S. A., 1974, *ApJ*, 187, 333
 Cusumano G., et al., 2006a, *GCN* 4775
 Cusumano G., et al., 2006b, *GCN* 4786
 Dai Z. G., Lu T., 1998, *MNRAS*, 298, 87
 De Luca A., 2006, *GCN* 4853
 Fan Y. Z., Piran T., 2006, *MNRAS*, in press (astro-ph/0601054)
 Frail D. A., et al., 2001, *ApJ*, 562, L55
 Halpern J. P., Kemp J., Piran T., Bershadsky M. A., 1999, *ApJ*, 517, L105
 Huang Y. F., Cheng K. S., Gao T. T., 2006, *ApJ*, 637, 873
 Li Z. Y., Chevalier R. A., 1999, *ApJ*, 526, 716
 Mészáros P., Rees M. J., Wijers R. A. M. J., 1998, *ApJ*, 499, 301
 Mirabal N. et al., 2006, *ApJL*, submitted (astro-ph/0603686)
 Mirabal N., Halpern J. P., 2006, *GCN* 4792
 Modjaz M., et al., 2006, *ApJL*, submitted (astro-ph/0603377)
 Nousek J., et al., 2006, *GCN* 4805
 Panaitescu A., & Kumar P., 2001, *ApJ*, 560, L49
 Pian E., et al., 2006, *Nature*, submitted (astro-ph/0603530)
 Piran T., 1999, *Phys. Rep.*, 314, 575
 Piran T., Kumar P., Panaitescu A., Piro L., 2001, *ApJ*, 560, L167
 Ramirez-ruiz E., Celotti A., & Rees M. J., 2002, *MNRAS*, 337, 1349
 Rhoads, J. E. 1999, *ApJ*, 525, 737
 Sakamoto T., et al., 2006, *GCN* 4822
 Sari R., Narayan R., Piran T., 1996, *ApJ*, 473, 204
 Sari R., Piran T., Narayan R. 1998, *ApJ*, 497, L17
 Sari R., Piran T., Halpern J. P., 1999, *ApJ*, 519, L17
 Soderberg A., et al. 2006, *ApJ*, 638, 930
 Sollerman J., et al., 2006, *A&A*, submitted (astro-ph/0603495)
 Waxman E., 2004, *ApJ*, 605, L97
 Wei D. M., Lu T., 1998, *ApJ*, 505, 252
 Woosley S. E., Zhang W. Q., Heger A., 2003, *AIPC*, 662, 185
 Yost S., Harrison F. A., Sari R., Frail D. A., 2003, *ApJ*, 597, 459
 Zhang W. Q., Woosley S. E., Heger A., 2004, *ApJ*, 608, 305